scientific reports

Check for updates

OPEN

# Establishment and characterization of mouse metabolic dysfunction-associated steatohepatitis-related hepatocellular carcinoma organoids

Sumin Kim[1,2,6], Nahyun Jeong[1,2,6], Jeayeon Park[3], Hyojin Noh[3], Ja Oh Lee[1,2], Su Jong Yu[3]✉ & Ja-Lok Ku[1,2,4,5]✉

**Metabolic dysfunction-associated steatohepatitis (MASH) is a form of chronic liver inflammation associated with metabolic syndrome, such as obesity and a major cause of hepatocellular carcinoma (HCC). Multi-biotics, a soymilk fermented with lactic acid bacteria, are known to alleviate obesity by lowering lipid profile. This study aimed to establish and characterize mouse organoids derived from MASH-related HCC models to evaluate drug responses, particularly focusing on Lenvatinib resistance. Organoids were developed using mouse liver tissues subjected to a choline-deficient L-amino acid-defined high-fat diet (CDAHFD) to mimic MASH-related HCC. The study evaluated the effect of multi-biotics, a fermented product, on tumor regression and drug sensitivity. While multi-biotics did not reduce tumor burden, they enhanced the response to Lenvatinib. Additionally, repeated treatment with Lenvatinib led to the development of drug-resistant organoids. Transcriptomic analysis of these resistant organoids identified key pathways related to KRAS signaling, inflammation, and epithelial-mesenchymal transition (EMT), revealing potential targets for overcoming Lenvatinib resistance. This study provides valuable insights into MASH-related HCC progression and drug resistance, offering a model for further therapeutic research.**

**Keywords** Hepatocellular carcinoma (HCC), Metabolic dysfunction-associated steatohepatitis (MASH), Organoid, Lenvatinib, Multi-biotics, Choline-deficient L-amino acid-defined high-fat diet (CDAHFD)

Hepatocellular carcinoma (HCC) is the most common primary liver cancer, accounting for approximately 90% of liver cancer cases and ranking as the third leading cause of cancer-related deaths worldwide[1,2]. Among the various risk factors for HCC, metabolic dysfunction-associated steatohepatitis (MASH), also known as non-alcoholic steatohepatitis (NASH), has rapidly emerged as a significant contributor to HCC incidence[3,4]. MASH is characterized by chronic liver inflammation, which can progress to fibrosis, cirrhosis, and ultimately HCC[5,6]. Recent studies have employed various mouse models to explore the pathogenesis of MASH-related HCC, with the choline-deficient L-amino acid-defined high-fat diet (CDAHFD) mouse model proving particularly effective due to its rapid and severe induction of MASH and HCC[7–9].

Given the rising prevalence of MASH-related HCC, there is a critical need for effective treatment strategies. Multi-biotics, a product derived from the fermentation of soy protein with kimchi and lactic acid bacteria, have shown promise in alleviating obesity by lowering the levels of low-density lipoprotein cholesterol through the partial suppression of adipocyte differentiation[10]. Additionally, Lenvatinib, a multi-target tyrosine kinase inhibitor (TKI), is currently used as a first-line treatment for HCC[11,12], primarily targeting receptor tyrosine

[1]Korean Cell Line Bank, Laboratory of Cell Biology, Cancer Research Institute, Seoul National University College of Medicine, Seoul 03080, Korea. [2]Cancer Research Institute, Seoul National University, Seoul 03080, Korea. [3]Department of Internal Medicine and Liver Research Institute, Seoul National University College of Medicine, Seoul 03080, Republic of Korea. [4]Department of Biomedical Sciences, Seoul National University College of Medicine, Seoul 03080, Korea. [5]Ischemic/Hypoxic Disease Institute, Seoul National University College of Medicine, Seoul 03080, Korea. [6]Sumin Kim and Nahyun Jeong contributed equally. ✉email: ydoctor2@snu.ac.kr; kujalok@snu.ac.kr

kinases involved in angiogenesis and cell proliferation[13,14]. However, resistance to Lenvatinib remains a significant challenge, limiting its long-term efficacy in treating HCC[15,16].

This study aimed to establish and characterize organoids derived from mouse models of normal liver and MASH-related HCC to assess the efficacy of multi-biotics and the drug response profiles of these organoids, particularly focusing on Lenvatinib resistance. We first established mouse MASH-HCC organoids and evaluated the effects of multi-biotics on tumor regression, finding that multi-biotics did not significantly reduce tumor burden. Subsequent RNA sequencing of MASH-HCC organoids treated with multi-biotics revealed distinct transcriptomic features, including differentially expressed genes associated with lipid metabolism and inflammation.

Drug sensitivity testing of the organoids against four FDA-approved HCC treatments—Cabozantinib, Lenvatinib, Regorafenib, and Sorafenib—demonstrated that multi-biotics enhanced the response of MASH-HCC organoids to Lenvatinib. To further investigate Lenvatinib resistance, we developed Lenvatinib-resistant MASH-HCC organoids through repeated drug administration. Transcriptomic analysis of these resistant organoids identified enriched pathways related to KRAS signaling, inflammatory responses, and epithelial-mesenchymal transition, highlighting potential mechanisms underlying resistance.

In summary, our study provides a comprehensive model for studying MASH-related HCC and Lenvatinib resistance using organoid technology. These findings offer valuable insights into the molecular mechanisms of drug resistance in MASH-HCC and suggest potential therapeutic targets for overcoming resistance, thereby advancing the development of more effective treatments for HCC.

## Results

### Establishment of normal mouse liver organoid and MASH-related HCC Mouse Organoids

To evaluate the effect of multi-biotics on tumor regression, physiological characteristics were examined in three mouse model groups. The negative control group was fed a commercial standard diet (SD), the positive control group was fed a CDAHFD and the multi-biotics group was fed CDAHFD with multi-biotics. The results indicated that multi-biotics exhibited no reduction on body and liver weight and the ratio of liver/body weight (Supplementary Fig. S1a-d). Additionally, there was no significant difference in nodule count between the positive control group and the multi-biotics group (Supplementary Fig. S1e). Changes in biochemical markers were examined in plasma obtained from three groups: negative control, positive control, and multi-biotics. ALT, AST, ALP, and total bilirubin were significantly increased in the positive control and multi-biotics groups compared to the negative control group. On the other hand, triglyceride was slightly decreased in both groups, but there was no significant difference (Supplementary Fig. S1f).

To determine whether multi-biotics affect the reduction of hepatic steatosis in MASH-HCC, oil red-O staining was performed. Increased lipid accumulation was confirmed in the positive control and multi-biotics groups at early and late stages (Supplementary Fig. S2a). However, in the late stage, the multi-biotics group showed relatively reduced lipid accumulation compared to the positive control group, whereas no significant difference was observed in the early stage (Supplementary Fig. S2b). When nonalcoholic fatty liver disease (NAFLD) activity score was examined, in both early and late stages, there was a statistically significant difference in the NAFLD Activity Score (NAS) between the positive control and multi-biotics groups, with lower NAS values observed in the multi-biotics group (Supplementary Fig. S2c). Taken together, administration of multi-biotics did not affect tumor regression in MASH-HCC, but did affect the reduction of hepatic steatosis.

To further characterize MASH-HCC with multi-biotics, we established organoids using tissues from the mouse MASH-HCC model. When analyzing the morphology of the mouse liver organoids, all organoids predominantly exhibited a cystic form (Fig. 1a). The histopathological characteristics of the tumor organoids and tissues were confirmed through H&E staining. The results showed tumors formed in the liver tissues and also revealed a high fat content in tumor tissues derived from HCC caused by MASH (Fig. 1b and Supplementary Fig. S3). Furthermore, the expression of C/EBP α, a hepatocyte marker, and α Fetoprotein (AFP), a liver cancer marker, was assessed in organoids using immunocytochemistry. C/EBPα and AFP were similarly expressed in the positive controls and multi-biotics organoids (Supplementary Fig. S4a, b).

We also investigated transcriptomic differences between positive control group and multi-biotics group using RNA-sequencing. As a results, 456 differentially expressed genes (DEGs) were significantly identified ($|Log2FC| > 1$, $padj < 0.05$), and the expression of the top 30 gene set based on padj, including Slc5a8, Ltf, Rps4l, Vnn3, and Mcm5, was confirmed (Supplementary Table S1 and Fig. 1c).

### Drug sensitivity of mouse liver normal and HCC organoids

Drug screening was conducted to assess drug responsiveness in the established mouse liver organoids. The drug library were constructed using the list of Food and Drug Administration (FDA)-approved HCC drugs provided by the National Cancer Institute (NCI), which included Cabozantinib, Lenvatinib, Regorafenib, and Sorafenib. The viability of organoids treated with these four drugs was evaluated across nine different drug concentrations (Fig. 2a-d and Supplementary Table S2). Sensitivity to each drug was determined based on the area under the curve (AUC), which was calculated from the cell viability curve (Supplementary Table S3 and Supplementary Fig. S5).

The positive control group exhibit comparable response to Lenvatinib only (Supplementary Fig. S5). SNU-6621-TO and SNU-6622-TO showed variable responses to Cabozantinib, Sorafenib and Regorafenib. In the multi-biotics group, samples showed similar reactivity to all drugs. Both samples of the multi-biotics groups were sensitive to Sorafenib, Cabozantinib, and Lenvatinib, but resistant to Regorafenib. These data indicated that, unlike other drugs, the response to Lenvatinib differed significantly between the positive control and multi-

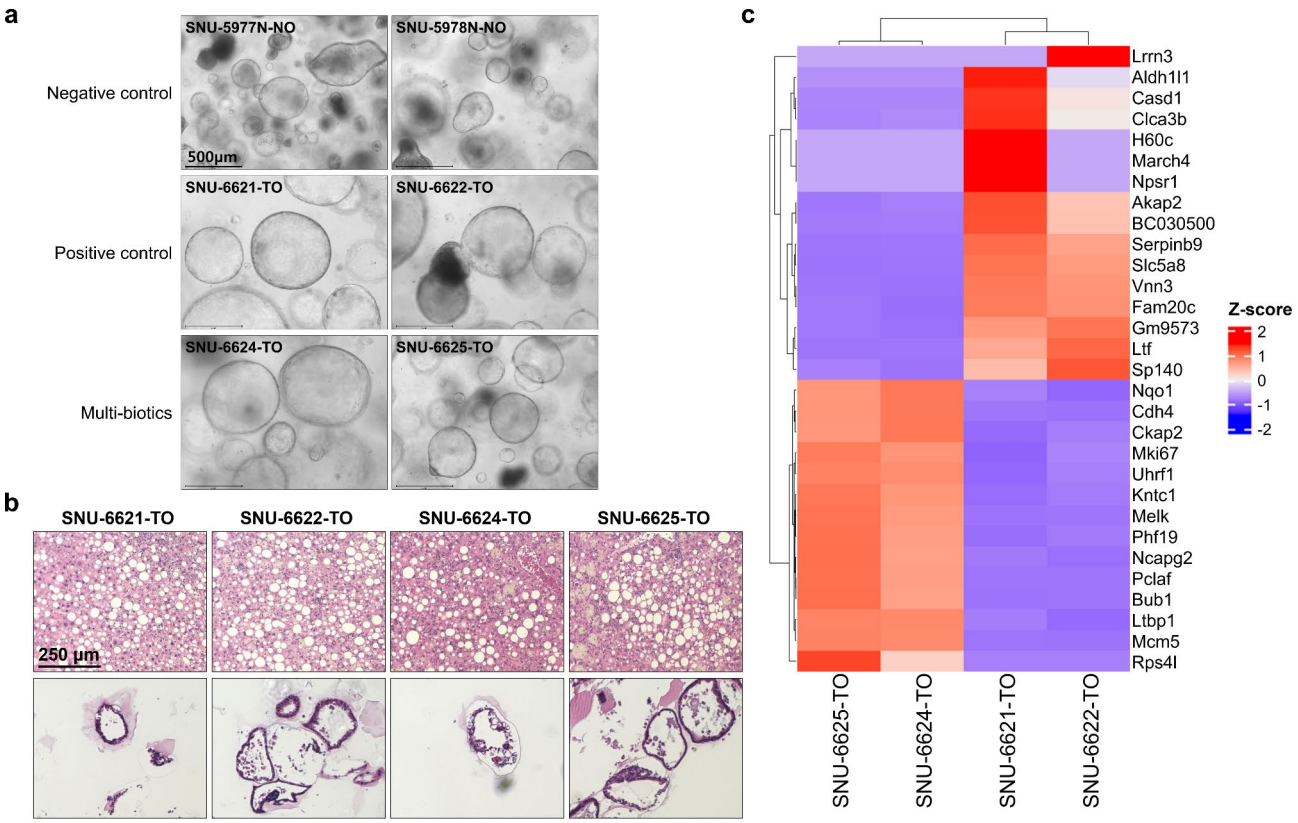


**Fig. 1**. Characterization of Mouse Organoids (**a**) The morphology of mouse normal liver and MASH-HCC organoids is depicted. Negative control group is normal organoids, positive control group is MASH-related HCC organoids, and multi-biotics group is MASH-related HCC organoids treated multi-biotics. Scale bar = 500 μm. (**b**) H&E staining of mouse MASH-HCC tissues and organoids is shown. Scale bar = 250 μm. (**c**) The expression of differentially expressed genes (DEGs) between the positive control and multi-biotics groups.

biotics groups and multi-biotics have a potential association with reactivity of Lenvatinib than other drugs. Taken together, these findings suggest that multi-biotics exclusively improved the response to Lenvatinib.

## Establishment of Lenvatinib-resistant MASH-related HCC organoids

We previously identified that the group treated with multi-biotics showed a good response to Lenvatinib. Subsequently, we investigated the changes that would occur with repeated administration of Lenvatinib.

The MASH-HCC organoids were treated repeatedly with the half-maximal inhibitory concentration (IC50) value of Lenvatinib. Unlike the second treatment, the morphology observed after the third treatment was similar to that before treatment with Lenvatinib. However, when Lenvatinib was administered at increased concentrations (20 μM), the morphology of the organoids deteriorated. Interestingly, after one more treatment with 20 μM of Lenvatinib (5th treatment), the morphology reverted to a state similar to that before treatment with Lenvatinib (Fig. 3a and Supplementary Fig. S6a).

To confirm whether this morphological change was due to resistance to Lenvatinib, drug responsiveness was assessed. The resistance model, in which Lenvatinib was administered five times repeatedly, showed decrease in cytotoxic effect of Lenvatinib (Fig. 3b, c and Supplementary Fig. S6b, c). In the multi-biotics group, the IC50 in the resistance model increased more than fifteen times compared to the parent model that was not treated with Lenvatinib (Supplementary Table S4). These results suggest that repeated treatment with Lenvatinib in the multi-biotics group induced resistance.

## Transcriptomic analysis of Lenvatinib-resistant MASH-related HCC treated with multi-biotics

To determine the changes that occurred when MASH-HCC treated with multi-biotics responded to Lenvatinib, we performed transcriptomic analyses. In the multi-biotics group treated with Lenvatinib, 1,548 DEGs were identified ($|Log2FC| > 2$, $padj < 0.05$; Supplementary Table S5). The enriched pathways included adipogenesis, IL-2-STAT5 signaling, and upregulated KRAS signaling (Supplementary Table S6 and Fig. 4a, b).

When resistance to Lenvatinib developed, we examined the transcriptomic features in the multi-biotics group. As a result, 486 DEGs were found in the multi-biotics group that developed Lenvatinib resistance ($|Log2FC| > 1$, $padj < 0.05$; Supplementary Table S7). The enriched pathways included the inflammatory response, TNF-α

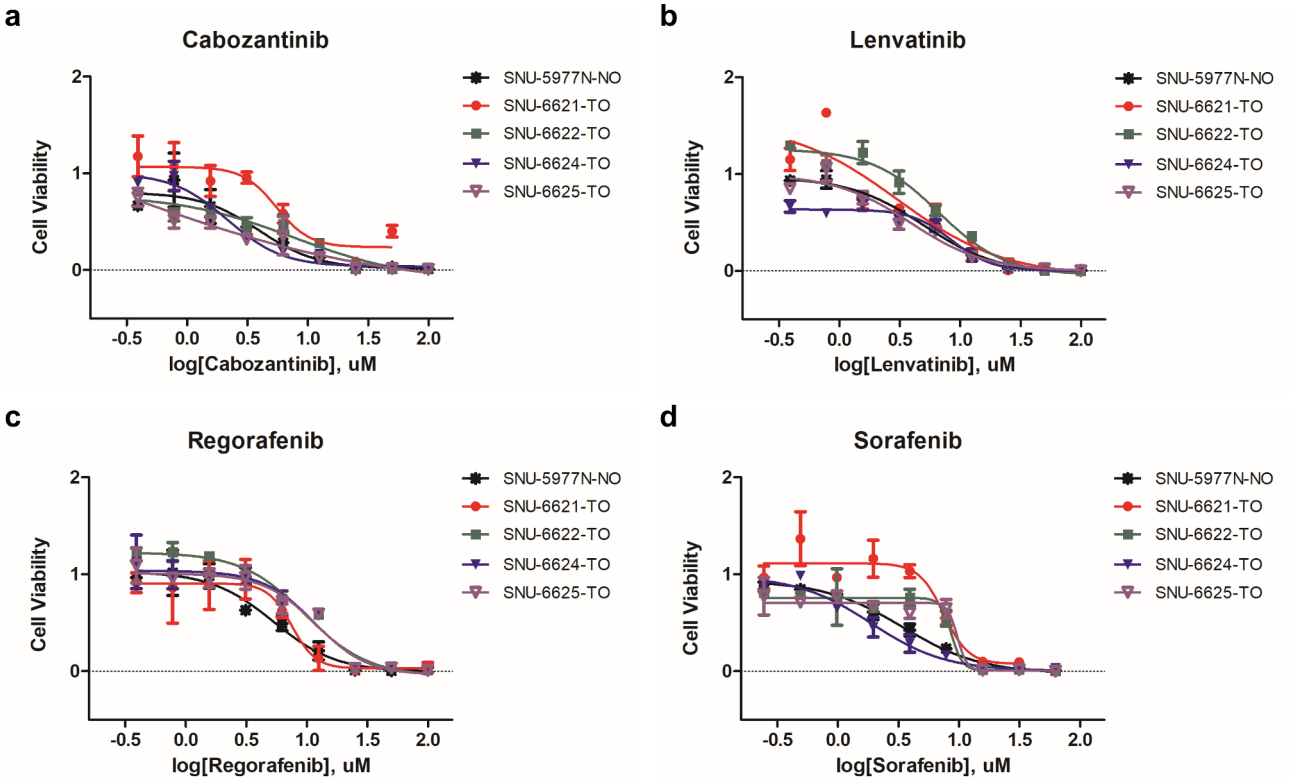


**Fig. 2**. Heterogeneous Drug Responses of Mouse Liver Organoids to Four FDA-Approved Liver Cancer Drugs. The cell viability curves of mouse liver organoids in response to (**a**) Cabozantinib, (**b**) Lenvatinib, (**c**) Regorafenib, and (**d**) Sorafenib are illustrated.

signaling via NF-κB, upregulated KRAS signaling, and epithelial-mesenchymal transition (EMT; Supplementary Table S8 and Fig. 4c, d).

Next, we speculated that genes commonly regulated in the group treated with Lenvatinib and the group that developed Lenvatinib resistance were related to responsiveness to Lenvatinib. To determine if there were genes simultaneously regulated in both groups, we compared the DEGs that appeared when the multi-biotics group was treated with Lenvatinib and those that appeared when Lenvatinib resistance developed. There were 145 genes that were commonly downregulated in both groups, and 12 genes that were upregulated (Fig. 4e, f). Among the commonly downregulated genes, Itga7 was related to adipogenesis. Among the commonly upregulated genes, Col7a1 was related to EMT, and Slpi was associated with the upregulated KRAS signaling pathway. Therefore, we suggest that these genes have the potential to be candidates for targeting resistance to Lenvatinib in MASH-HCC.

## Discussion

In our study, the primary goal was to establish and characterize mouse metabolic dysfunction-associated steatohepatitis (MASH)-related hepatocellular carcinoma (HCC) organoids, which serve as models for drug sensitivity and resistance studies. To establish MASH-HCC organoids, we developed MASH-HCC mouse models.

There are many previous studies on how to establish these MASH or MASH-HCC mouse models, and we established the MASH-HCC mouse model by feeding choline-deficient L-amino acid-defined high-fat diet (CDAHFD) to mice for 30 weeks. According to previous papers, when CDAHFD was fed to mice for 6 weeks, hepatic steatosis was induced, and when it was continued for 36 weeks, it could even induce HCC[17,18]. In our paper, we confirmed that MASH-related HCC was induced when CDAHFD was fed for 30 weeks. In addition, biochemical markers identified in the previous papers had similar regulation patterns.

Within this framework, we evaluated the effects of multi-biotics on MASH-HCC organoids, specifically in relation to their response to Lenvatinib. While multi-biotics were initially investigated for their potential role in modulating primary resistance to Lenvatinib, our findings revealed that although multi-biotics enhanced sensitivity to Lenvatinib, the development of secondary or acquired resistance was still inevitable, similar to what was observed in the untreated organoids.

Based on our findings, we observed that multi-biotics enhanced the initial response of MASH-HCC organoids to Lenvatinib compared to the control group. This suggests that multi-biotics may modulate pathways that improve sensitivity to Lenvatinib, which could potentially delay or reduce the onset of drug resistance. Future

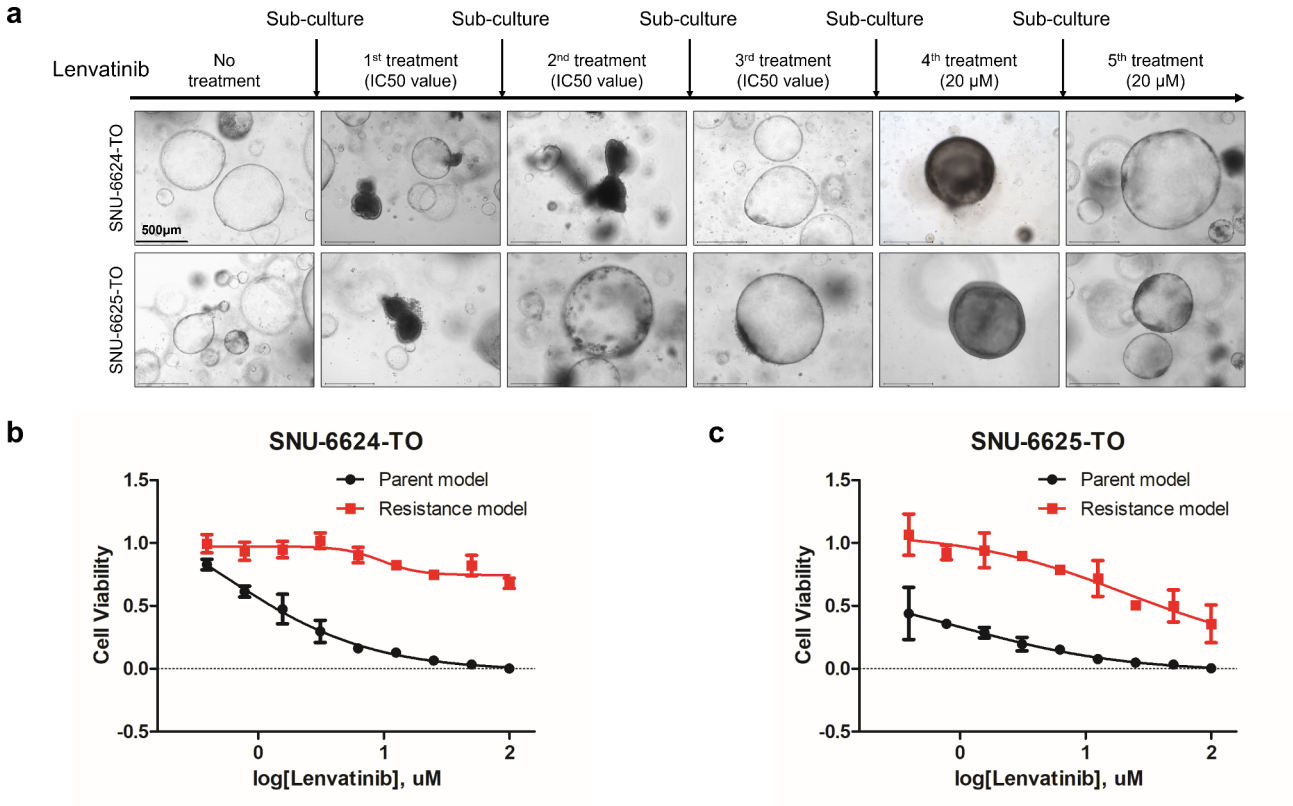


**Fig. 3**. Establishment of Lenvatinib-Resistant MASH-HCC Organoids in the Multi-Biotics Group. (**a**) The morphology of organoids at each stage of Lenvatinib treatment during the process of establishing Lenvatinib-resistant organoids. In the 1st treatment, 2nd treatment, and 3rd treatment, each sample was treated with the IC50 value of Lenvatinib. IC50 of SNU-6624-TO is 8.51 μM, and IC50 of SNU-6625-TO is 3.90 μM. Scale bars represent 500 μm. (b and c) Drug sensitivity to Lenvatinib for each set of parent HCC organoids and Lenvatinib-resistant MASH-HCC organoids. Black lines represent parent models and red lines represent Lenvatinib-resistant models. (**b**) SNU-6624-TO set. (**c**) SNU-6625-TO set.

studies could build on these findings by incorporating multi-biotics during repeated Lenvatinib treatments to investigate whether it could reduce the rate or extent of resistance development.

We performed RNA-sequencing to identify transcriptomic differences between the positive control and multi-biotics groups, and identified 30 DEGs between the two groups. Among these genes, several have been previously implicated in metabolic regulation and cancer biology. For instance, Slc5a8, which is significantly upregulated, has been shown to act as a tumor suppressor by facilitating the transport of short-chain fatty acids, thus modulating metabolic pathways in cancer cells[19,20]. Additionally, Vnn3 and Mcm5 are associated with cell proliferation and inflammatory responses, suggesting that the differences between the positive control and multi-biotics groups may be linked to alterations in metabolic and immune-related pathways[21,22]. In particular, pathways such as adipogenesis and IL-2-STAT5 signaling, which were enriched in multi-biotics-treated samples, may play a crucial role in modulating the response of organoids to Lenvatinib by influencing tumor cell growth and survival under treatment conditions. These transcriptomic differences underscore the potential role of multi-biotics in modulating these processes, although additional functional validation is needed to clarify their precise contributions.

The enriched pathways—such as inflammatory response, TNF-α signaling via NF-κB, upregulated KRAS signaling, and epithelial-mesenchymal transition (EMT)—are well-established mechanisms involved in cancer progression and therapy resistance. Specifically, the activation of NF-κB signaling pathway have been widely reported to contribute to resistance by promoting survival and proliferation in various cancer types, including HCC[23,24]. Moreover, EMT is a key process driving metastasis and resistance to targeted therapies, including Lenvatinib[25,26].

Previous studies have demonstrated that ABCB1, through the STAT3-ACB1 signaling axis, plays a crucial role in mediating drug resistance in HCC, particularly in relation to tyrosine kinase inhibitors like Lenvatinib[11]. Preliminary data suggests that the pathways we have identified could indeed intersect with the signaling networks associated with these markers, but additional validation at the protein level is essential. For example, assessing phosphorylation levels of ERK (MAPK pathway) and STAT3 could provide direct evidence linking these pathways to the observed resistance phenotypes.

Itga7 (integrin alpha-7), which we found to be downregulated in the Lenvatinib-resistant group, has been linked to adipogenesis and cellular adhesion processes. Integrins are crucial in mediating extracellular matrix

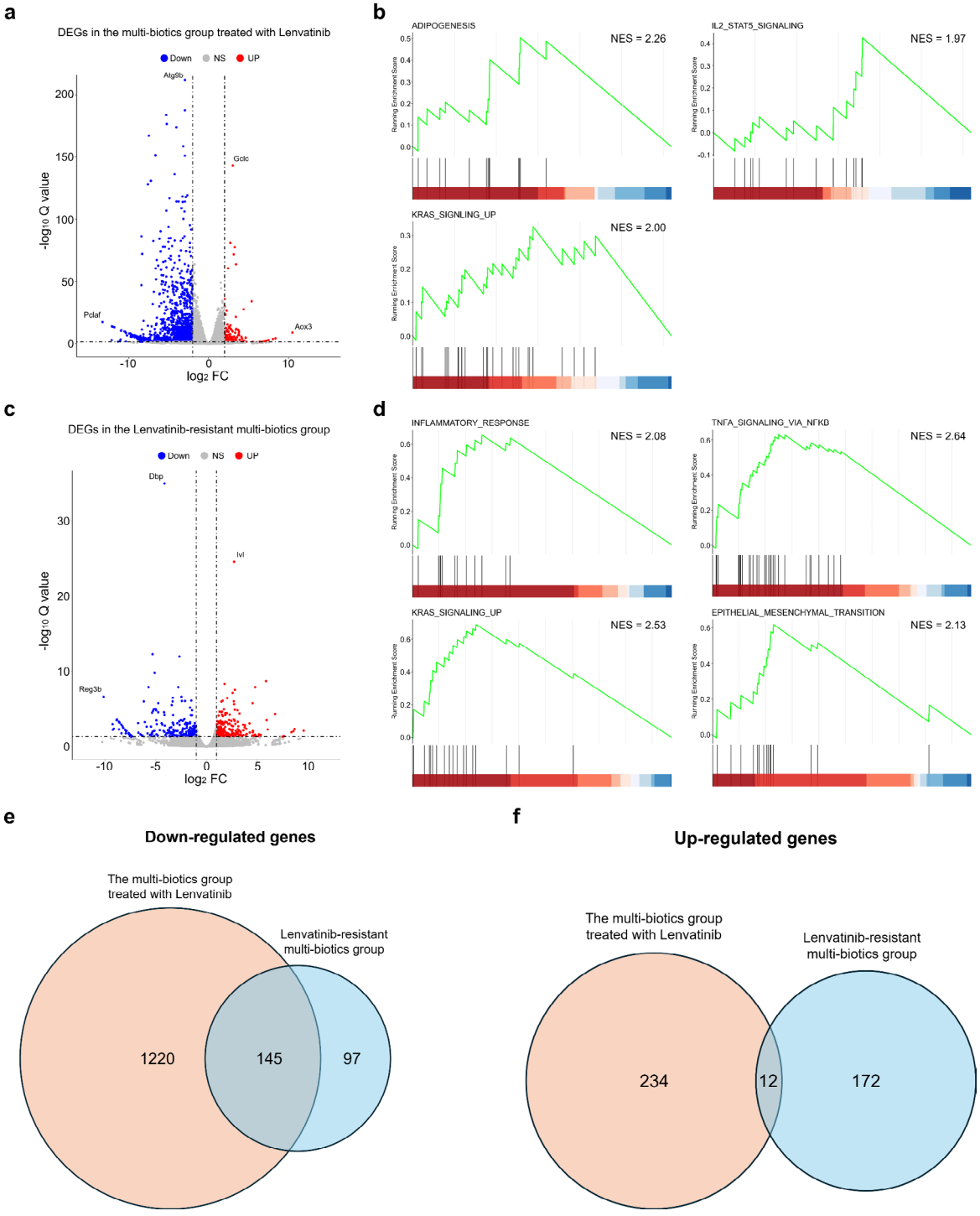


**Fig. 4**. Transcriptomic Analysis of MASH-Related HCC Treated with Multi-Biotics in Response to Lenvatinib. (**a**) Volcano plot of DEGs in the multi-biotics group treated with Lenvatinib compared to the multi-biotics group not treated with Lenvatinib. Red dots and blue dots represent up-regulated and down-regulated genes, respectively, while gray dots represent non-significant genes ($|Log2FC| > 2$, $padj < 0.05$). Genes with the highest Log2FoldChange and the lowest padj in both down-regulation and up-regulation are labeled. (**b**) Hallmark pathways enriched in the multi-biotics group treated with Lenvatinib. (**c**) Volcano plot of DEGs in the Lenvatinib-resistant multi-biotics group compared to the parent multi-biotics group. Red dots and blue dots represent up-regulated and down-regulated genes, respectively, while gray dots represent non-significant genes ($|Log2FC| > 1$, $padj < 0.05$). Genes with the highest Log2FoldChange and the lowest padj in both down-regulation and up-regulation are labeled. (**d**) Hallmark pathways enriched in the Lenvatinib-resistant multi-biotics group. (e and f) Venn diagrams of (**e**) down-regulated genes and (**f**) up-regulated genes between the multi-biotics group treated with Lenvatinib and the Lenvatinib-resistant multi-biotics group.

(ECM) interactions, and a loss of function in these proteins can disrupt the ECM, leading to changes in cellular adhesion, migration, and signaling[27]. In the context of adipogenesis, Itga7 downregulation may contribute to a metabolic shift that supports tumor progression and resistance by enhancing tumor cell survival under Lenvatinib treatment. This shift could reduce the tumor's reliance on normal metabolic pathways, making it less susceptible to anti-angiogenic therapies like Lenvatinib, which target nutrient supply.

Col7a1 (collagen type VII alpha 1), which was upregulated in the resistant group, plays a key role in the EMT process[28]. EMT is known to drive metastasis and drug resistance in many cancers, including HCC. Col7a1 upregulation can contribute to the EMT process by promoting changes in cellular structure and mobility, thereby enhancing the ability of tumor cells to evade Lenvatinib's inhibitory effects on cell proliferation. EMT is also linked to resistance by increasing the plasticity of cancer cells, enabling them to adapt to and survive therapeutic pressures.

Slpi (secretory leukocyte protease inhibitor), associated with KRAS signaling, was also upregulated in the Lenvatinib-resistant group. KRAS is a well-established driver of oncogenic signaling, and Slpi has been shown to enhance cellular proliferation and survival through the upregulation of protease inhibitors that protect cells from apoptosis[29]. The upregulation of Slpi could therefore contribute to Lenvatinib resistance by sustaining KRAS-driven signaling pathways that support cell growth and survival, despite the drug's anti-proliferative effects.

These genes (Itga7, Col7a1, and Slpi) are not only key players in processes such as adipogenesis, EMT, and KRAS signaling but also present potential therapeutic targets. Targeting these pathways could reverse or mitigate resistance mechanisms, making them important candidates for further study in the context of overcoming Lenvatinib resistance. Future studies aimed at validating the roles of these genes, potentially through protein-level assessments and functional assays, would provide a more comprehensive understanding of their involvement in resistance.

This study provides novel insights into the effects of multi-biotics on MASH-related HCC and drug resistance, specifically Lenvatinib resistance, using mouse-derived organoid models. Our results demonstrate that while multi-biotics did not significantly reduce tumor burden in the MASH-HCC mouse model, they did enhance the response of HCC organoids to Lenvatinib, a first-line treatment for HCC. This finding suggests that multi-biotics may modulate cellular pathways that affect drug sensitivity, representing a potential adjunct therapy to enhance the efficacy of existing cancer treatments.

The establishment of MASH-related HCC organoids and their characterization are critical steps toward understanding the cellular and molecular dynamics of MASH-HCC, especially in the context of drug resistance. Organoids derived from mouse models fed a CDAHFD closely mimic the human disease state, offering a valuable platform for investigating the pathogenesis of MASH and its progression to HCC. These organoids also allow for high-throughput drug screening and the study of tumor biology in a controlled environment that retains the heterogeneity of primary tumors.

Our study's most significant contribution is the establishment of Lenvatinib-resistant MASH-related HCC organoids and the identification of transcriptomic changes associated with resistance. By repeatedly administering Lenvatinib to MASH-HCC organoids, we observed morphological and viability changes indicative of resistance development. Transcriptomic analysis revealed that resistant organoids exhibited enriched pathways related to inflammation, KRAS signaling, and EMT. These findings underscore the complex interplay between drug treatment and cellular adaptation, which drives resistance and highlights potential targets for overcoming it.

The enhanced response of MASH-HCC organoids to Lenvatinib in the presence of multi-biotics is particularly noteworthy. Our data suggest that multi-biotics may influence key signaling pathways, such as those involved in cell proliferation and survival, thereby sensitizing the cells to Lenvatinib. The identification of differentially expressed genes, such as Slpi and Col7a1, which are associated with KRAS signaling and EMT, provides a potential mechanistic explanation for the observed drug sensitivity. These genes represent promising targets for further investigation as they may play a role in modulating the tumor microenvironment and influencing drug response.

The implications of these findings extend beyond MASH-related HCC, offering broader relevance to other cancers where drug resistance poses a significant challenge. The use of multi-biotics, which combine the benefits of prebiotics, probiotics, and postbiotics, may offer a novel approach to modulate the gut-liver axis and influence systemic metabolism, potentially impacting tumor biology. This highlights the importance of exploring dietary and microbial interventions as complementary strategies in cancer therapy, particularly in enhancing the efficacy of conventional treatments like Lenvatinib.

Furthermore, this study provides a foundation for future research aimed at integrating multi-biotics into combination therapy regimens. The observed enhancement of Lenvatinib response by multi-biotics suggests that similar approaches could be applied to other therapeutic agents, potentially broadening the scope of treatment options for patients with drug-resistant HCC. Additionally, understanding the specific components of multi-biotics that contribute to this effect could lead to the development of more targeted adjunct therapies.

The use of organoid models in this study also highlights the potential of patient-derived organoids as a personalized medicine tool. By generating organoids from individual patients with MASH-related HCC, it may be possible to predict responses to multi-biotics and other interventions, thus tailoring treatment strategies to individual patients' unique genetic and molecular profiles.

While the findings of this study are promising, there are limitations that should be addressed in future research. The reliance on mouse models, while informative, may not fully capture the genetic diversity and complexity of human HCC. Thus, validating these results in human-derived organoids and clinical samples will be crucial to confirm the translatability of our findings. Additionally, exploring the effects of multi-biotics on other signaling pathways involved in drug resistance, as well as expanding the range of therapeutic agents tested, will provide a more comprehensive understanding of their potential benefits.

In conclusion, this study underscores the novelty and importance of using multi-biotics as a potential adjunct therapy to enhance drug response in MASH-related HCC. The establishment of Lenvatinib-resistant organoids provides a valuable tool for studying resistance mechanisms and testing new treatment strategies. These findings pave the way for future research exploring the integration of dietary and microbial interventions in cancer therapy, ultimately aiming to improve outcomes for patients with drug-resistant tumors. The ability of multi-biotics to modulate key pathways and enhance drug efficacy highlights a promising avenue for overcoming the persistent challenge of cancer drug resistance.

## Materials and methods

### Animal and study design

Male C57BL/6 mice, specified as pathogen-free and aged 5 weeks, underwent a one-week adaptation phase. The mice were randomly divided into three groups ($n = 8$/group/each experimental time-point); the negative control group was fed a commercial standard diet (SD); the positive control group was fed a choline-deficient, L-amino acid- defined, high-fat diet (CDAHFD) with 0.1% methionine (CDAHFD; #A06071302, Research Diets, New Brunswick, NJ, USA); and the treatment group was fed CDAHFD with Multi-biotics. The experimental group was fed the same CDAHFD but also received Multi-biotics at a dosage of 3 mg per mouse per day, mixed in their food, along with sterile water diluted at 1/1000. MASH-HCC was induced in C57BL/6 mice by feeding a CDAHFD for 30 weeks. Multi-biotics treatment was started simultaneously with CDAHFD feeding and continued for the entire study duration. All animal experiments in this study were conducted according to a protocol approved by the Institutional Animal Care and Committee of Seoul National University Hospital (approval no:19-0083-S1A2) and were in accordance with the ARRIVE guidelines.

### Multi-biotics

Multi-biotics, Soypro™, is a product that ferments soy protein with kimchi and milk lactic acid bacteria, then freeze-dries the mixture for preservation and health benefits[10]. Multi-biotics contain 12 different types of lactic acid bacteria, including 4 strains of milk lactic acid bacteria and 8 strains of kimchi lactic acid bacteria. The postbiotics in Multi-biotics include various fermented natural products.

### Sampling

At 8 and 30 weeks, mice were euthanized by exsanguination under isoflurane anesthesia. Blood samples were collected from the abdominal aorta of mice in each group and centrifuged at 300 × g for 15 min. Serum aliquots (0.8 mL) were stored in Eppendorf tubes at -80 °C until analysis. Immediately following the death of the mice, their livers were swiftly removed and photographed. Subsequently, the livers were weighed, and the hepatic index (i.e., liver weight (g) per mouse body weight (kg)) was calculated. A portion of the liver tissue was then immediately fixed in 4% neutral-buffered formalin for histological analysis. The severity and size of lesions such as steatosis, inflammation, ballooning, and fibrosis in the liver were assessed.

### Histopathological assessment

Liver tissues from mice were collected for the purpose of metabolite analysis. A portion of the samples were fixed in a formalin solution, then embedded in paraffin. Paraffin-embedded tissue samples were cut into 4-μm-thick sections, deparaffinized in xylene, and dehydrated through a graded series of ethanol solutions. For detailed histological assessment, sections were stained using three distinct staining techniques: hematoxylin and eosin (H&E) and Oil Red O (ORO).

### Non-alcoholic fatty liver disease activity score

An experienced pathologist assessed the stained liver sections using the non-alcoholic fatty liver disease activity score (NAS) developed by the NASH Clinical Research Network[30]. This score incorporates evaluations of steatosis, lobular inflammation, and hepatocyte ballooning. Steatosis is graded based on the proportion of hepatocytes exhibiting fat accumulation, with categories reflecting none, less than one-third, one-third to two-thirds, and more than two-thirds affected. Lobular inflammation is quantified by the number of inflammatory foci per 200x microscopic field, identifying the range from none to more than four foci. Hepatocyte ballooning assesses the presence of swollen, damaged hepatocytes with rarefied cytoplasm, indicative of cell stress or injury, and is scored based on the extent and prominence of ballooning cells. The combined scores of these three parameters create a composite NAS, which ranges from 0 to 8; a higher NAS suggests the presence of NASH.

### Organoid sample preparation

Organoids were established using the liver tissue of normal and MASH-HCC mice. These mouse liver tissues were initially rinsed with ice-cold PBS before being finely chopped. The tissue was then subjected to dissociation into single cells using a digestion medium comprising collagenase and hyaluronidase in a DMEM/F12 solution. This mixture was incubated at 37 °C for 40 min with intermittent shaking. The resulting single cells were filtered through a 100 μm cell strainer. After this, the cells were centrifuged at 1500 rpm for 3 min. The cells were then washed in a solution containing 5% Bovine Calf Serum (BCS) in DMEM/F12 medium, followed by centrifugation at 1500 rpm for 3 min to obtain a cell pellet.

### Establishment of MASH-related murine HCC organoids

The dissociated tumor cell pellet was suspended in Basement Membrane Extract (BME) (Cultrex® PC BME RGF Type 2, Aimbio), and the suspension was seeded onto a flat-bottomed plate. The BME gel was allowed to polymerize in a $CO_2$ incubator for 15 min, following which the Liver Expansion medium was added for

organoid culture. During the initial 48 h, 10 µL of Y-27,632 was added to the Liver Expansion medium, which was subsequently replaced with the standard Liver Expansion medium. The Liver Expansion medium is formulated with 50% (v/v) L-WRN conditioned medium, 50 ng/mL human EGF, 100 ng/mL human FGF, 10 mM Nicotinamide, 1× B27 supplement, 1× N2 supplement, 1 mM N-Acetyl-L-cysteine, 10 nM Gastrin, 10 µM Forskolin, and 100 µg/mL Primocin in Basal culture medium. The Basal culture medium contains 10 mM GlutaMAX, 100 U/mL penicillin, 100 µg/mL streptomycin, and 10% (v/v) FBS in DMEM/F12. The culture medium was refreshed every three to five days. For passaging, the culture medium and BME were removed, and BME dissolution was facilitated by adding 10 mL of TrypLE Express (Invitrogen). The cell pellet was resuspended in BME, and the cells were seeded in droplets of 50–100 µL each. After polymerization of the BME gel, the Liver Expansion medium was added for further organoid culture. All organoids were maintained in a humidified incubator at 37 °C with 5% $CO_2$. Organoids developed in this study are under the governance and distribution of Dr. Ku Ja-Lok and the Korean Cell Line Bank (KCLB) for global sharing.

## H&E staining

Tumor tissues were preserved in 10% neutral buffered formalin and subsequently embedded in paraffin. These tissues were then sectioned to a thickness of 4 µm. In the case of organoids, the BME dome was gently scraped using a pipette tip. To collect the dissociated BME domes, 10 mL of cold PBS was added and then transferred into a 15 mL conical tube. The tube was centrifuged at 100 rpm for 15 s, after which the supernatant was carefully removed. This process was repeated until the BME gel was completely detached, ensuring the preservation of the organoids' structural integrity. The harvested organoids were then embedded in 2% agarose gel. The solidified agarose gel was fixed in 10% formalin for 30 min at room temperature and sectioned to a thickness of 4 µm. These sections were then processed for Hematoxylin and Eosin (H&E) staining.

## Immunocytochemistry

The fixation and permeabilization were carried out using BD Cytofix/Cytoperm™ (BD Science, CA, USA). The organoids were then washed with a solution provided by BD Science and incubated for one hour in 0.1% PBS.T containing 3% FBS (GE Healthcare Life Sciences, Buckinghamshire, UK) for blocking. Following this, organoids were washed again with 0.1% PBS.T and incubated with C/EBP α antibody (1:500, Santa Cruz Biotechnology, Texas, USA) and α Fetoprotein antibody (1:100, Abcam, Cambridge, United Kingdom) for over-night at 4℃. After washing with 0.1% PBS.T, Alexa 488 secondary antibodies (1:500, Thermo Fisher Scientific, MA, USA) diluted in 0.1% PBS.T, were applied for one hour at room temperature. For nuclear and actin filament staining, 1× DAPI and Rhodamine-conjugated Phalloidin (1:10, Sigma-Aldrich, MO, USA) were diluted in DPBS and applied for 40 min at room temperature. The organoids were washed three times with DPBS and then imaged using an LSM800 Confocal Laser Scanning Microscope with ZEN software (Carl Zeiss, Oberkochen, Germany).

## Organoid drug sensitivity test

To obtain single cells, organoids were dissociated with BME both enzymatically and mechanically, which involved incubation and pipetting in TrypLE Express solution for 10 min. Following the dissolution of the BME, the cell suspension (5 µL per well) was dispensed into clear-bottomed, white-walled 96-well plates. This was then covered with 60 µL of a 1:1 mixture of the Liver Expansion medium and RGF basement membrane matrix (Gibco, A14132-02). The plates were incubated at 37 °C in a 5% $CO_2$ environment for 15 min to allow the gel to solidify, followed by the addition of 20 µL of the Liver Expansion medium to each well. 96 h post-seeding, 20 µL of the solution containing the drug was added to each well. Within the Liver Expansion medium, the drugs were serially diluted in a 1:2 ratio starting from the maximum dose, resulting in nine different concentration levels. For the control group, a combination of Liver Expansion medium and drug-solvent solution was added to all plates.

## ATP detection assay

Seventy-two hours following drug administration, 10 µL of CellTiter-Glo 3D Reagent (Promega #G968B) was added to each well, followed by 5 min of intensive shaking. The CellTiter-Glo 3D Reagent was used to quantify ATP levels, which directly correlate with metabolically active, viable cells. The mixture was then incubated at room temperature for 30 min, followed by an additional minute of shaking, before measuring luminescence using a Luminoskan Ascent (Thermo Fisher Scientific, MA, USA) with an integration time of 1000 milliseconds. The data were normalized against the vehicle control, and IC50 values were calculated using GraphPad Prism 5. For the graphs representing cell viability, the arbitrary units from 0 to 1 shown in the figures reflect the normalized luminescence values relative to the vehicle control. The luminescence signal from treated wells was divided by that from the vehicle control wells (set as 1) to construct the dose-response curves.

## Establishment of Lenvatinib-resistant murine MASH-related HCC organoids

Organoids were initially cultured in 24-well plates and allowed to stabilize over 7 days. Subsequently, the organoids were maintained by treating the culture medium with Lenvatinib for 7 days, after which the medium was replaced with the Lenvatinib-free culture medium. This was incubated for an additional 7 days, and the subculturing process was repeated until resistance to Lenvatinib developed (Supplementary Fig. S7). This cumulative drug treatment approach was adopted based on methodologies outlined in previously published literature[31]. For the first three-drug treatment cycles, the IC50 value of Lenvatinib specific to each organoid was utilized. In the fourth cycle, concentrations of 5 µM, 10 µM, and 20 µM Lenvatinib were employed, culminating in a final treatment with 20 µM Lenvatinib. For generating Lenvatinib-resistant organoids, we used 5 µM, 10 µM, and 20 µM Lenvatinib in sequential treatment rounds to ensure robust selection pressure and induce resistance

over time. This approach, while exceeding the initial IC50, was designed to progressively challenge the cells and mimic clinical conditions where higher drug concentrations might be encountered.

### RNA-sequencing

In this study, the experimental groups used for RNA-sequencing were divided into four groups: a positive control group, a multi-biotics group, a multi-biotics group treated with Lenvatinib, and a Lenvatinib-resistant multi-biotics group. The first positive control group was MASH-HCC organoids that were not treated with anything, and the second multi-biotics group was MASH-HCC organoids treated with multi-biotics. The third Lenvatinib-treated multi-biotics group was the multi-biotics group treated with Lenvatinib once, and the fourth Lenvatinib-resistant multi-biotics group was the multi-biotics group treated with Lenvatinib five times to develop Lenvatinib resistance.

Total RNA was isolated from cell lysate using Trizol (Qiagen) and Qiagen RNeasy Kit (Qiagen). Sequencing libraries were prepared using the Illumina TruSeq Stranded mRNA LT Sample Prep Kit. Paired end sequencing reads of cDNA libraries (101 bp) generated from a NovaSeq6000 instrument were verified its sequence quality with FastQC v 0.11.7. For data preprocessing, low quality bases and adapter sequences in reads were trimmed using Trimmomatic 0.38. The trimmed reads were aligned to the genomic reference (mm10) using HISAT2 v2.1.0 through Bowtie2 aligner (v2.3.4.1). Then, transcript assembly of known transcripts and genes was processed by StringTie v2.1.3b. Based on the result, expression abundance of transcript and gene were calculated as read count or fragments per kilobase of exon per million fragments mapped (FPKM) and Transcripts Per Kilobase Million (TPM) value per sample.

### Statistics analysis

Statistical analyses were performed using the R software (version 4.3.1). Analysis of DEGs was carried out utilizing the DEseq2 package. Additionally, pathway analyses were conducted employing various software packages, including ggplot2 and clusterProfiler.

## Data availability

Organoids generated in this study have been deposited to the Korean Cell Line Bank (KCLB, http://cellbank.snu.ac.kr, http://organoid.snu.ac.kr) biobank and are governed by Ja-Lok Ku. The datasets analysed during the current study are available in the Gene Expression Omnibus (GEO) repository, the primary accession code GSE272024 (https://www.ncbi.nlm.nih.gov/geo/query/acc.cgi? acc=GSE272024).

Received: 24 July 2024; Accepted: 5 November 2024
Published online: 10 November 2024

## References

1. Villanueva, A. & Hepatocellular Carcinoma *N Engl. J. Med.* **380**, 1450–1462 https://doi.org/10.1056/NEJMra1713263 (2019).
2. Pinter, M., Pinato, D. J., Ramadori, P. & Heikenwalder, M. NASH and Hepatocellular Carcinoma: Immunology and Immunotherapy. *Clin. Cancer Res.* **29**, 513–520. https://doi.org/10.1158/1078-0432.Ccr-21-1258 (2023).
3. Teng, M. L. P. et al. Global incidence and prevalence of nonalcoholic fatty liver disease. *Clin. Mol. Hepatol.* **29**, 32–S42. https://doi.org/10.3350/cmh.2022.0365 (2023).
4. Huang, D. Q. et al. Changing global epidemiology of liver cancer from 2010 to 2019: NASH is the fastest growing cause of liver cancer. *Cell Metabol.* **34**, 969–977e962. https://doi.org/10.1016/j.cmet.2022.05.003 (2022).
5. Kutlu, O., Kaleli, H. N. & Ozer, E. Molecular pathogenesis of nonalcoholic Steatohepatitis- (NASH-) related Hepatocellular Carcinoma. *Can. J. Gastroenterol. Hepatol.* **2018** (8543763). https://doi.org/10.1155/2018/8543763 (2018).
6. Yoon, E. L. & Jun, D. W. Waiting for the changes after the adoption of steatotic liver disease. *Clin. Mol. Hepatol.* **29**, 844–850. https://doi.org/10.3350/cmh.2023.0291 (2023).
7. Febbraio, M. A. et al. Preclinical models for studying NASH-Driven HCC: how useful are they? *Cell. Metab.* **29**, 18–26. https://doi.org/10.1016/j.cmet.2018.10.012 (2019).
8. Ikawa-Yoshida, A. et al. Hepatocellular carcinoma in a mouse model fed a choline-deficient, L-amino acid-defined, high-fat diet. *Int. J. Exp. Pathol.* **98**, 221–233. https://doi.org/10.1111/iep.12240 (2017).
9. Matsumoto, M. et al. An improved mouse model that rapidly develops fibrosis in non-alcoholic steatohepatitis. *Int. J. Exp. Pathol.* **94**, 93–103. https://doi.org/10.1111/iep.12008 (2013).
10. Kim, N. H. et al. Lipid profile lowering effect of SoyproTM fermented with lactic acid bacteria isolated from Kimchi in high-fat diet-induced obese rats. *BioFactors.* **33**, 49–60. https://doi.org/10.1002/biof.5520330105 (2008).
11. Hu, B. et al. Inhibition of EGFR overcomes acquired Lenvatinib Resistance Driven by STAT3-ABCB1 signaling in Hepatocellular Carcinoma. *Cancer Res.* **82**, 3845–3857. https://doi.org/10.1158/0008-5472.CAN-21-4140 (2022).
12. Wang, L. et al. METTL3-m6A-EGFR-axis drives lenvatinib resistance in hepatocellular carcinoma. *Cancer Lett.* **559**, 216122. https://doi.org/10.1016/j.canlet.2023.216122 (2023). https://doi.org/https://doi.org/
13. Zhao, Y., Zhang, Y. N., Wang, K. T. & Chen, L. Lenvatinib for hepatocellular carcinoma: from preclinical mechanisms to anti-cancer therapy. *Biochim. Biophys. Acta Rev. Cancer.* **1874**, 188391. https://doi.org/10.1016/j.bbcan.2020.188391 (2020).
14. Tan, W. et al. GPX2 is a potential therapeutic target to induce cell apoptosis in lenvatinib against hepatocellular carcinoma. *J. Adv. Res.* **44**, 173–183. https://doi.org/10.1016/j.jare.2022.03.012 (2023).
15. He, X. et al. EGFR inhibition reverses resistance to lenvatinib in hepatocellular carcinoma cells. *Sci. Rep.* **12**, 8007. https://doi.org/10.1038/s41598-022-12076-w (2022).
16. Fu, R., Jiang, S., Li, J., Chen, H. & Zhang, X. Activation of the HGF/c-MET axis promotes lenvatinib resistance in hepatocellular carcinoma cells with high c-MET expression. *Med. Oncol.* **37**, 24. https://doi.org/10.1007/s12032-020-01350-4 (2020).
17. Nababan, S. et al. Choline-deficient high-fat Diet-induced Steatohepatitis in BALB/c mice. *Mol. Cell. Biomedical Sci.* **5**, 74. https://doi.org/10.21705/mcbs.v5i2.193 (2021).
18. Ikawa-Yoshida, A. et al. Hepatocellular carcinoma in a mouse model fed a choline-deficient, L-amino acid-defined, high-fat diet. *Int. J. Exp. Pathol.* **98**, 221–233. https://doi.org/10.1111/iep.12240 (2017).
19. Li, H. et al. SLC5A8, a sodium transporter, is a tumor suppressor gene silenced by methylation in human colon aberrant crypt foci and cancers. *Proc. Natl. Acad. Sci. U S A.* **100**, 8412–8417. https://doi.org/10.1073/pnas.1430846100 (2003).

20. Vargas-Sierra, O. et al. Role of SLC5A8 as a tumor suppressor in Cervical Cancer. *Front. Biosci. (Landmark Ed).* **29**, 16. https://doi.org/10.31083/j.fbl2901016 (2024).
21. Ha, M. et al. VNN3 is a potential novel biomarker for predicting prognosis in clear cell renal cell carcinoma. *Anim. Cells Syst. (Seoul).* **23**, 112–117. https://doi.org/10.1080/19768354.2019.1583126 (2019).
22. Zhou, J. et al. MCM5 is a Novel Therapeutic Target for Glioblastoma. *Onco Targets Ther.* **17**, 371–381. https://doi.org/10.2147/ott.S457600 (2024).
23. Xia, Y., Shen, S. & Verma, I. M. NF-κB, an active player in human cancers. *Cancer Immunol. Res.* **2**, 823–830. https://doi.org/10.1158/2326-6066.Cir-14-0112 (2014).
24. Lin, Y., Bai, L., Chen, W. & Xu, S. The NF-kappaB activation pathways, emerging molecular targets for cancer prevention and therapy. *Expert Opin. Ther. Targets.* **14**, 45–55. https://doi.org/10.1517/14728220903431069 (2010).
25. Qin, Y. et al. Lenvatinib in hepatocellular carcinoma: resistance mechanisms and strategies for improved efficacy. *Liver Int.* **44**, 1808–1831. https://doi.org/10.1111/liv.15953 (2024).
26. Huang, Y., Hong, W. & Wei, X. The molecular mechanisms and therapeutic strategies of EMT in tumor progression and metastasis. *J. Hematol. Oncol.* **15**, 129. https://doi.org/10.1186/s13045-022-01347-8 (2022).
27. Hamidi, H. & Ivaska, J. Author correction: every step of the way: integrins in cancer progression and metastasis. *Nat. Rev. Cancer.* **19**, 179. https://doi.org/10.1038/s41568-019-0112-1 (2019).
28. Ding, C. et al. Collagen type VII α1 chain: a promising prognostic and immune infiltration biomarker of pancreatic cancer. *Oncol. Lett.* **25**, 77. https://doi.org/10.3892/ol.2023.13663 (2023).
29. Zhang, X., Liu, S. S., Ma, J. & Qu, W. Secretory leukocyte protease inhibitor (SLPI) in cancer pathophysiology: mechanisms of action and clinical implications. *Pathol. Res. Pract.* **248**, 154633. https://doi.org/10.1016/j.prp.2023.154633 (2023).
30. Kleiner, D. E. et al. Design and validation of a histological scoring system for nonalcoholic fatty liver disease. *Hepatology.* **41**, 1313–1321. https://doi.org/10.1002/hep.20701 (2005).
31. Coley, H. M. in *In Cancer Cell Culture: Methods and Protocols*. 267–273 (eds Langdon, S. P.) (Humana, 2004).


## Acknowledgements

This research was funded and supported by National Research Foundation of Korea (grant nos. 2021M3H9A1030151, NRF2022R1A5A102641311, 2022M3A9B6018217). Biospecimens and data used in this study were provided by the Biobank of Seoul National University Hospital, a member of the Korea Biobank Network.

## Author contributions

S.M.K and N.H.J : conceptualization, methodology, resources, formal analysis, data curation, software, visualization, validation, investigation, and writing – original draft. J.Y.P and H.J.N : methodology, resources, visualization, and writing – review and editing. J.O.L : investigation, and resources. S.J.Y and J.-L.K : resources, project administration, writing – review and editing, funding acquisition, and supervision.

## Declarations

## Competing interests

The authors declare no competing interests.

## Additional information

**Supplementary Information** The online version contains supplementary material available at https://doi.org/10.1038/s41598-024-78963-6.

**Correspondence** and requests for materials should be addressed to S.J.Y. or J.-L.K.